Anti-Windup Predictive Control for an Engine Air Path System

Ikuro Mizumoto * **Yusuke Makimoto** **

* *Faculty of Advanced Science and Technology, Kumamoto University, Kumamoto, Japan (e-mail: ikuro@gpo.kumamoto-u.ac.jp)*
** *Department of Mechanical System Eng., Kumamoto University, Kumamoto, Japan*

Abstract: This paper deals with the control problem of an engine air path system with the air mass flow and EGR rate as the outputs and throttle valve and EGR valve as inputs. In the considered system, since the EGR response is slow compared with the response of the intake air mass, the overshoot and undershoot phenomena occur in fresh air mass flow during transient response. Moreover, the mechanical restriction of the valves opening range results in instability of the control system. In this paper, we propose an anti-windup predictive control taking into inputs restriction for air path system to improve transient performance and to maintain the stable air path system.

Keywords: output predictor, output predictive control, parallel feedforward compensator, anti-windup control

1. INTRODUCTION

The combustion engine technologies have been highly developed during recent decade due to requirements of high combustion efficiency and low emission. The exhaust gas recirculation (EGR) is one of the effective ways to improve the combustion efficiency. It is expected to reduce the nitrogen oxide (NOx) and intake loss by adding the engine air path system such as EGR. Unfortunately, however, the slow response due to transport delay of gas flow from EGR causes over intake fresh air in the intake manifold. This affect fuel consumption and/or ride quality of the automobile. The advanced control is effective way to bringing out the ability of the air path system. As well known, most conventional control technique for engines have been based on the feedforward controls by the look-up tables, which are so called ‘control maps’. However, since engine system have higher nonlinearities and might be sensitive to disturbances and the change of environment, developing the control maps for feedforward control requires a lot of time and effort with number of experiments to obtain in-depth data in order to make an accurate control map. Therefore, advanced control strategies, which is robust with respect to changes of environment and disturbances for engine control, have attracted a great deal of attention in order to keep robust and stable combustion during the operation, and have strongly expected to achieve high-performance of engine control.

The model predictive controls (MPC) are well recognized as one of the effective control strategies in industrial fields (Clarke et al., 1987; Garcia et al., 1989). This control method is also expected to apply the engine air path control and have been researched actively in recent decade as a control strategy for air path system of engines (Herceg et al., 2006; Ferreau et al., 2007; Ortner et al., 2009; Gelso and Lindberg, 2014; Kekik and Akar, 2020, 2019). However, in order to apply the MPC for nonlinear system having some constraints, nonlinear optimization problem and/or quadratic programing (QP) problem have to be solved online. This might be restriction to apply the MPC method to engine air path control. Moreover, the application of the MPC is based on the applicability of the accurate model of the considered controlled system.

Recently, an output prediction based robust predictive control strategy was proposed for both discrete-time and continuous-time systems (Mizumoto et al., 2015, 2018). Unlike the conventional MPC methods, this method can design predictive control without solving QP problem on line. However, the method did not handle the systems with input constrains.

In this paper, we consider applying the predictive control method in Mizumoto et al. (2018) to engine air path system with input saturation. The method in Mizumoto et al. (2018) is extended to deal with input saturation without solving nonlinear optimization problem. To this end, a novel anti-windup control for predictive control will be provided in this paper. In the proposed method, an extended virtual ideal system, which can estimate the output of the ideal system without input saturation, is considered and the predictive control is provided without solving nonlinear optimization problem online. The effectiveness of the proposed method is also confirmed through numerical simulations.

2. MODEL OF ENGINE AIR PATH SYSTEM

The considered engine air path system in this paper is illustrated as in Fig. 1. The variables and parameters in the engine model are defined as in Table. 1.

In this engine air path system, we suppose that the air mass m_{imo} in the intake manifold and EGR ratio r_{egr} are

Table 1. List of variables and parameters in the Air Path Model

Symbol	Description
Variables	
$\dot{m}_{th}$	Throttle mass flow [kg/s]
$\dot{m}_{egr}$	EGR mass flow [kg/s]
$\dot{m}_z$	Cylinder mass flow [kg/s]
p_{im}	Intake manifold pressure [Pa]
F_{im}	O2 fraction of intake manifold [-]
m_{im}	Gas mass in intake manifold [kg]
m_{imo}	Air(02) mass in intake manifold [kg]
r_{egr}	EGR ratio [-]
θ_{th}	Throttle valve angle [deg]
θ_{EGR}	EGR valve angle [deg]
A_{th}	Effective opening area of the throttle valve [m^2]
A_{EGR}	Effective opening area of the EGR valve [m^2]
Constants	
p_a	Ambient pressure [Pa]
p_{em}	Pressure at EGR valve[Pa]
F_{air}	O2 fraction of air [Pa]
F_{em}	O2 fraction of exhaust gas [Pa]
V_{im}	Volume of intake manifold [m^3]
V_s	Volume of each cylinder [m^3]
T_{im}	Temperature of intake manifold [K]
R_a	Specific gas constant [J/(kgK)]
κ	Specific heat ratio [-]
n	Polytropic index [-]
ω_e	Engine speed [rpm]
η_v	Cylinder efficiency [-]

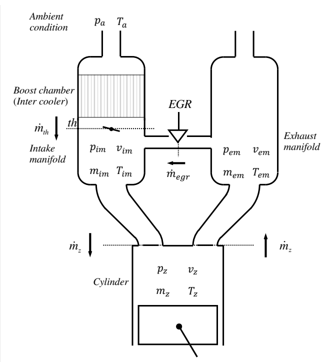

Fig. 1. Air Path System

referred as outputs of the system, and the throttle valve angle θ_{th} and EGR valve angle θ_{EGR} are considered as input of the system. The followings are the model of the air path system according to the physical relations.

The air mass in the intake manifold m_{imo} is obtained from the gas mass in the intake manifold as

$$m_{imo} = m_{im} \times (1 - r_{egr}(t)) \tag{1}$$

$$m_{im} = \frac{p_{im}V_{im}}{R_a T_{im}} \tag{2}$$

The EGR ratio is defined and obtained from the O_2 fraction of air and O_2 fraction in the intake manifold by

$$r_{egr}(t) = 1 - \frac{\bar{F}_{im}(t)}{F_{air}} \tag{3}$$

and

$$\dot{F}_{im} = \frac{R_a T_{im}}{p_{im} V_{im}} \{(F_{air} - F_{im})\dot{m}_{th} + (F_{em} - F_{im})\dot{m}_{egr}\} \tag{4}$$

Moreover, mass flow $\dot{m}_{th}$ at the throttle valve, mass flow $\dot{m}_{egr}$ at the EGR valve and mass flow $\dot{m}_z$ at the cylinder are obtained by

$$\dot{m}_{th} = A_{th}(\theta_{th})U(p_a)\Phi(p_{im}, p_a) \tag{5}$$

$$\dot{m}_{egr} = A_{egr}(\theta_{egr})U(p_{em})\Phi(p_{im}, p_{em}) \tag{6}$$

$$\dot{m}_z = \frac{\omega_e p_{im} V_s \eta_v}{120 R_a T_{im}} \tag{7}$$

Where $A_{th}(\theta_{th})$ and $A_{egr}(\theta_{egr})$ are the effective opening area of the throttle valve and EGR valve respectively with $A(\theta)$ defined by

$$A(\theta) = A_{max}\{1 - \cos(\theta)\} \tag{8}$$

and $U(p)$ and $\Phi(p_2, p_1)$ are nonlinear functions defined by

$$U(p) = \sqrt{2p\rho} \tag{9}$$

$$\Phi(p_2, p_1) = \begin{cases} \sqrt{\dfrac{\kappa}{\kappa - 1}\left\{\left(\dfrac{p_2}{p_1}\right)^{\frac{2}{\kappa}} - \left(\dfrac{p_2}{p_1}\right)^{\frac{\kappa+1}{\kappa}}\right\}} \\ \left(\left(\dfrac{p_2}{p_1}\right) > \left(\dfrac{2}{\kappa+1}\right)^{\frac{\kappa}{\kappa-1}}\right) \\ \left(\dfrac{2}{\kappa+1}\right)^{\frac{1}{\kappa-1}} \sqrt{\dfrac{\kappa}{\kappa+1}} \\ \left(\left(\dfrac{p_2}{p_1}\right) \leq \left(\dfrac{2}{\kappa+1}\right)^{\frac{\kappa}{\kappa-1}}\right) \end{cases} \tag{10}$$

Where ρ represents the density.

In this model, we assume that the temperature in the air path system is constant of T_{im}, and thus we have the following relation concerning the pressure of the intake manifold.

$$\dot{p}_{im} = \frac{n R_a T_{im}}{V_{im}} (\dot{m}_{th} + \dot{m}_{egr} - \dot{m}_z) \tag{11}$$

For the detailed about the modeling of the combustion engine system, refer Guzzella and Onder (2020).

It should be noted that we supposed that there is a delay elements in the EGR air path system due to transport delay. Therefore, an unknown higher order delay elements will be added to the above derived model as a model for the illustrative example shown in the following Section 4.

3. PROBLEM STATEMENT

Consider designing a control system for two-input/two-output engine air path system with the outputs of the air mass m_{imo} in the intake manifold and EGR ratio r_{egr}, and the inputs of the throttle valve angle θ_{th} and EGR valve angle θ_{egr}.

We suppose that the nominal linear model at a basis running point of engine is known as follows.

$$G(s) = \begin{bmatrix} G_{11}(s) & G_{12}(s) \\ G_{21}(s) & G_{22}(s) \end{bmatrix} \tag{12}$$

Moreover, the system can be modelled by the following dicentralized state space model:

$$\begin{aligned} \dot{\boldsymbol{x}}_i(t) &= A_{ii}\boldsymbol{x}_i(t) + \boldsymbol{w}_i(t) + b_i u_i(t) \\ y_i(t) &= \boldsymbol{c}_i^T \boldsymbol{x}_i(t) \end{aligned} \tag{13}$$

$$\boldsymbol{w}_i(t) = \sum_{j=1}^{2} B_{ij}\boldsymbol{x}_j(t), \quad B_{ij} = \begin{cases} O & , \ i = j \\ A_{ij} & , \ i \neq j \end{cases} \tag{14}$$

$$i = 1, 2$$

Where $i = 1$ represents the system from $u_1(t) = \theta_{th}$ to $y_1(t) = m_{imo}$ and $i = 2$ represents the system from $u_2(t) = \theta_{egr}$ to $y_2(t) = r_{egr}$.

Suppose that for the nominal model (13), suppose that the following assumption is satisfied.

Assumption 1. For the system:

$$\begin{aligned} \dot{\boldsymbol{x}}_i(t) &= A_{ii}\boldsymbol{x}_i(t) + b_i u_i(t) \\ y_i(t) &= \boldsymbol{c}_i^T \boldsymbol{x}_i(t) \end{aligned} \tag{15}$$

without interference term $\boldsymbol{w}_i(t)$ from the each subsystem given in (13), a parallel feedforward compensator (PFC):

$$\begin{aligned} \dot{\boldsymbol{x}}_{fp,i}(t) &= A_{fp,i}\boldsymbol{x}_{fp,i}(t) + \boldsymbol{b}_{fp,i}u_i(t) \\ y_{fp,i}(t) &= \boldsymbol{c}_{fp,i}^T\boldsymbol{x}_{fp,i}(t) \ , \end{aligned} \tag{16}$$

which makes the following augmented system having the PFC in parallel with the system (15)

$$\begin{aligned} \dot{\boldsymbol{x}}_{ap,i}(t) &= A_{ap,i}\boldsymbol{x}_{ap,i}(t) + \boldsymbol{b}_{ap,i}u_i(t) \\ y_{ap,i}(t) &= \boldsymbol{c}_{ap,i}^T\boldsymbol{x}_{ap,i}(t) \end{aligned} \tag{17}$$

$$\boldsymbol{x}_{ap,i}(t) = \begin{bmatrix} \boldsymbol{x}_i(t) \\ \boldsymbol{x}_{fp,i}(t) \end{bmatrix} \ , \ A_{ap,i} = \begin{bmatrix} A_{ii} & 0 \\ 0 & A_{fp,i} \end{bmatrix}$$

$$\boldsymbol{b}_{ap,i} = \begin{bmatrix} \boldsymbol{b}_i \\ \boldsymbol{b}_{fp,i} \end{bmatrix} \ , \ \boldsymbol{c}_{ap,i} = \begin{bmatrix} \boldsymbol{c}_i \\ \boldsymbol{c}_{fp,i} \end{bmatrix}$$

have relative degree of 1 and minimum-phase, is known.

Assumption 2. The saturated input applying the system can be modelled by

$$u_{R,i}(t) = \begin{cases} u_{lim,i}(t)\mathrm{sign}(u(t)) & |u_i(t)| > u_{lim,i} \\ u_i(t) & |u_i(t)| < u_{lim,i} \end{cases} \tag{18}$$

3.1 Anti-Windup Output Predictive Control

Based on the anti-windup strategy provided in Mizumoto and Momiki (2018), we propose an anti-windup predictive control method.

3.2 Output Estimator for Input Saturated System

Since the considered system satisfies Assumption 1, There exists a known PFC which renders the augmented system (17) having the relative degree of 1 and being minimum-phase. Thus for augmented system of the considered controlled system (13) with the PFC (16), there exists a nonsingular transformation $\begin{bmatrix} y_{ap,i}(t) & \boldsymbol{\eta}_i(t)^T \end{bmatrix}^T = \Phi\boldsymbol{x}_{ap,i}(t)$ such that the augmented system (17) can be transformed into the following canonical form (Isidori, 1995):

$$\begin{aligned} \dot{y}_{ap,i}(t) &= a_{a,i}^* y_{ap,i}(t) + b_{a,i}^* u_i(t) + \boldsymbol{c}_{\eta,i}^T\boldsymbol{\eta}_i(t) + \boldsymbol{d}_{w,i}^T\boldsymbol{w}_i(t) \\ \dot{\boldsymbol{\eta}}_i(t) &= A_{\eta,i}\boldsymbol{\eta}_i(t) + \boldsymbol{b}_{\eta,i}y_{ap,i}(t) + F_{w,i}\boldsymbol{w}_i(t) \end{aligned} \tag{19}$$

Moreover, denoting the nominal value of $a_{a,i}^*, b_{a,i}^*$ as $a_{a,i}, b_{a,i}$, the system can be represented by

$$\dot{y}_{ap,i}(t) = a_{a,i}y_{ap,i}(t) + b_{a,i}u_i(t) + f_i(t) \tag{20}$$

$$\begin{aligned} f_i(t) =& \Delta a_{a,i}y_{ap,i}(t) + \Delta b_{a,i}u_i(t) \\ &+ \boldsymbol{c}_{\eta,i}^T\boldsymbol{\eta}_i(t) + \boldsymbol{d}_{w,i}^T\boldsymbol{w}_i(t) \end{aligned} \tag{21}$$

with $\Delta a_{a,i} = a_{a,i}^* - a_{a,i}$, $\Delta b_{a,i} = b_{a,i}^* - b_{a,i}$.

Now, consider the case where the input saturation exists. The considered system is expressed as follows with saturated input $u_R(t)$ under Assumption 2.

$$\dot{y}_{ap,i}(t) = a_{a,i}y_{ap,i}(t) + b_{a,i}u_{R,i}(t) + f_i(t) \tag{22}$$

$$\begin{aligned} f_i(t) =& \Delta a_{a,i}y_{ap,i}(t) + \Delta b_{a,i}u_{R,i}(t) \\ &+ \boldsymbol{c}_{\eta,i}^T\boldsymbol{\eta}_i(t) + \boldsymbol{d}_{w,i}^T\boldsymbol{w}_i(t) \end{aligned} \tag{23}$$

For this system, consider the following stable filter:

$$\dot{y}_{aw,i}(t) = -a_{aw,i}y_{aw,i}(t) + b_{a,i}(-\Delta u_i(t)) \tag{24}$$

with $-\Delta u_i(t)$ as the input. Where $\Delta u_i(t) := u_{R,i}(t) - u_i(t)$.

Defining an auxiliary input $u_{aw,i}(t)$ by

$$u_{aw,i}(t) = -\frac{a_{a,i} + a_{aw,i}}{b_{a,i}}y_{aw,i}(t) = -k_{u,i}y_{aw,i}(t)$$

The filter (24) can be represented as follows:

$$\dot{y}_{aw,i}(t) = a_{a,i}y_{aw,i}(t) + b_{a,i}(u_{aw,i}(t) - \Delta u_i(t)) \tag{25}$$

Extending the system with the designed filter, it follows from (22) and (25) that

$$\begin{aligned} (\dot{y}_{ap,i}(t) + \dot{y}_{aw,i}(t)) &= a_{a,i}(y_{ap,i}(t) + y_{aw,i}(t)) \\ &+ b_{a,i}(u_{aw,i}(t) + u_i(t)) + f_i(t) \end{aligned} \tag{26}$$

By referring $u_{aw,i}(t) + u_i(t)$ as a control input, the extended system (26) is considered as the virtual ideal system without the input saturation given in (18). That is, the output $y_{ap,i}(t) + y_{aw,i}(t)$ represents the ideal output without input saturation and the filter output $y_{aw,i}(t)$ represents the missing signal in the system's output due to the input saturation. We call this filter 'Anti-Windup (AW) filter'.

Now, design the output estimator for the system (22) as

$$\begin{aligned} \dot{z}_{1,i}(t) =& a_{a,i}z_{1,i}(t) + b_{a,i}u_{Ri}(t) + z_{1,i}(t) \\ &+ k_{1,i}(y_{ap,i}(t) - z_{1,i}(t)) \end{aligned} \tag{27}$$

$$\dot{z}_{2,i}(t) = k_{2,i}(y_{ap,i}(t) - z_{1,i}(t)) \tag{28}$$

Where $z_{1,i}(t)$ is the estimated value of $y_{ap,i}(t)$ and $z_{2,i}(t)$ is the estimated value of $f_i(t)$. the design parameters $k_{1,i}$ and $k_{2,i}$ are set such that

$$A_{0,i} = \begin{bmatrix} a_{a,i} - k_{1,i} & 1 \\ -k_{2,i} & 0 \end{bmatrix} \tag{29}$$

is a stable matrix.

Using this output estimator, the estimated output of the extended virtual ideal system: is obtained by

$$\begin{aligned} (\dot{z}_{1,i}(t) + \dot{y}_{aw,i}(t)) &= a_{a,i}(z_{1,i}(t) + y_{aw,i}(t)) \\ &+ b_{a,i}(u_{aw,i}(t) + u_i(t)) + z_{2,i}(t) \\ &- k_{1,i}(z_{1,i}(t) - y_{ap,i}(t)) \end{aligned} \tag{30}$$

$$\dot{z}_{2,i}(t) = -k_{2,i}(z_{1,i}(t) - y_{ap,i}(t)) \tag{31}$$

Defining

$$\begin{aligned} \bar{y}_{ap,i}(t) &:= y_{ap,i}(t) + y_{aw,i}(t) \\ \bar{z}_{a1,i}(t) &:= z_{1,i}(t) + y_{aw,i}(t) \\ \bar{u}_i(t) &:= u_i(t) + u_{aw,i}(t) \end{aligned}$$

we finally obtain the following form of the output estimator for the the extended virtual ideal system:

$$\dot{\bar{z}}_{a1,i}(t) = a_{a,i}\bar{z}_{a1,i}(t) + b_{a,i}\bar{u}_i(t) + \bar{z}_{2,i}(t) - k_{1,i}(\bar{z}_{a1,i}(t) - \bar{y}_{ap,i}(t)) \tag{32}$$

$$\dot{\bar{z}}_{2,i}(t) = -k_{2,i}(\bar{z}_{a1,i}(t) - \bar{y}_{ap,i}(t)) \tag{33}$$

3.3 Output Predictor

Based on the form of designed output estimator (32), we consider the following output predictor from a current time t_0 for the extended virtual ideal system:

$$\dot{\hat{\bar{y}}}_{ap,i}(t) = a_{a,i}\hat{\bar{y}}_{ap,i}(t) + b_{a,i}\bar{v}_i(t) + \bar{z}_{2,i}(t_0) \tag{34}$$

$$\hat{\bar{y}}_{ap,i}(t_0) = \bar{z}_{1,i}(t_0) \quad , \quad t \geq t_0$$

Where $\bar{v}_i(t)$ is a predictive control input to be determined later.

It should be noted that the designed output predictor is the one for the augmented system with the given PFC (16).

From the structure of the augmented system (17), the predicted virtual ideal output for the practical system is obtained by

$$\begin{aligned}\hat{\bar{y}}_i(t) &= \hat{\bar{y}}_{ap,i}(t) - \bar{y}_{fp,i}(t) \\ &= \hat{\bar{y}}_{ap,i}(t) - c_{fp,i}^T\bar{\boldsymbol{x}}_{fp,i}(t) \\ &= \bar{c}_{ap,i}^T\bar{\boldsymbol{x}}_{ap,i}(t) \ ,\end{aligned} \tag{35}$$

with

$$\bar{\boldsymbol{x}}_{ap,i}(t) = \begin{bmatrix} \hat{\bar{y}}_{ap,i}(t) \\ \bar{\boldsymbol{x}}_{fp,i}(t) \end{bmatrix} \ , \ \bar{c}_{ap,i}^T = \begin{bmatrix} 1 \ , \ -c_{fp,i}^T \end{bmatrix}$$

where $\bar{\boldsymbol{x}}_{fp,i}(t)$ and $\bar{y}_{fp,i}(t)$ are the state and output of the PFC (16) with the input of $\bar{u}_i(t) := u_i(t) + u_{aw,i}(t)$, i.e.

$$\begin{aligned}\dot{\bar{\boldsymbol{x}}}_{fp,i}(t) &= A_{fp,i}\bar{\boldsymbol{x}}_{fp,i}(t) + b_{fp,i}\bar{u}(t) \\ \bar{y}_{fp,i}(t) &= \boldsymbol{c}_{fp,i}^T\bar{\boldsymbol{x}}_{fp,i}(t)\end{aligned} \tag{36}$$

The state equation of the defined $\bar{\boldsymbol{x}}_{ap,i}$-system can be expressed by

$$\dot{\bar{\boldsymbol{x}}}_{ap,i}(t) = \bar{A}_{ap,i}\bar{\boldsymbol{x}}_{ap,i}(t) + \bar{B}_{ap,i}\bar{\boldsymbol{v}}_{ap,i}(t) \tag{37}$$

with

$$\bar{A}_{ap,i} = \begin{bmatrix} a_{a,i} & O \\ O & A_{fp,i} \end{bmatrix} \ , \ \bar{B}_{ap,i} = \begin{bmatrix} b_{a,i} & 1 \\ b_{fp,i} & 0 \end{bmatrix}$$

$$\bar{\boldsymbol{v}}_{ap,i}(t) = \begin{bmatrix} \bar{v}_i(t) \\ \bar{z}_{2,i}(t_0) \end{bmatrix}$$

Using this output predictor we consider designing an output predictive controller based on the method provided in Mizumoto et al. (2018).

3.4 Output Predictive Controller Design

We consider to find a control input $\bar{v}(t)$ minimizing the following cost function J_i:

$$J_i = \frac{1}{2}\bar{\boldsymbol{x}}_{ap,i}^T(t_f)P_{f,i}\bar{\boldsymbol{x}}_{ap,i}(t_f) + \int_{t_0}^{t_f} \frac{1}{2}\left\{\hat{\bar{e}}_i(t)^2 + r_i\bar{v}_i(t)^2\right\}dt \tag{38}$$

$$\hat{\bar{e}}_i(t) = \hat{\bar{y}}_i(t) - y_{m,i}(t)$$

under the equality constrain in (37) and the following terminal constrain:

$$\begin{aligned}\hat{\bar{e}}_i(t_f) &= \hat{\bar{y}}_i(t_f) - y_{m,i}(t_f) \\ &= \bar{c}_{ap,i}^T\bar{\boldsymbol{x}}_{ap,i}(t_f) - y_{m,i}(t_f) = 0\end{aligned} \tag{39}$$

Where $P_{f,i} = P_{f,i} > 0$ and $r_i > 0$ are weights.

It is well recognized that the optimization problem for (38) can be solved from a optimization problem for the following cost function $\bar{J}_i$ by introducing Lagrange multipliers $\boldsymbol{\lambda}_i$, $\nu_{f,i}$:

$$\bar{J}_i = \varphi\left(\bar{\boldsymbol{x}}_{ap,i}(t_f), \nu_{f,i}, t_f\right) + \int_{t_0}^{t_f}\left(H\left(\bar{\boldsymbol{x}}_{ap,i}, \bar{v}, \boldsymbol{\lambda}_i, t\right) - \boldsymbol{\lambda}_i^T\dot{\bar{\boldsymbol{x}}}_{ap,i}(t)\right)dt \tag{40}$$

where

$$\varphi\left(\bar{\boldsymbol{x}}_{ap,i}(t_f), \nu_{f,i}, t_f\right) = \frac{1}{2}\bar{\boldsymbol{x}}_{ap,i}(t_f)^T P_{f,i}\bar{\boldsymbol{x}}_{ap,i}(t_f) + \nu_{f,i}\hat{\bar{e}}_i(t_f)$$

$$H\left(\bar{\boldsymbol{x}}_{ap,i}, \bar{v}_i, \boldsymbol{\lambda}_i, t\right) = \frac{1}{2}(\hat{\bar{e}}(t)^2 + r_i\bar{v}_i(t)^2) + \boldsymbol{\lambda}_i^T\left(\bar{A}_{ap,i}\bar{\boldsymbol{x}}_{ap,i}(t) + \bar{B}_{ap,i}\bar{\boldsymbol{v}}_{ap,i}(t)\right)$$

The optimization solution is obtained as the following Euler-Lagrange equation:

$$\dot{\bar{\boldsymbol{x}}}_{ap,i}(t) = \bar{A}_{ap,i}\bar{\boldsymbol{x}}_{ap,i}(t) + \bar{B}_{ap,i}\bar{\boldsymbol{v}}_i(t) \tag{41}$$

$$\bar{\boldsymbol{x}}_{ap,i}(t_0) = \begin{bmatrix} \hat{y}_{ap,i}(t_0) \\ \bar{\boldsymbol{x}}_{fp,i}(t_0) \end{bmatrix} \tag{42}$$

$$\dot{\boldsymbol{\lambda}}_i(t) = -\bar{\boldsymbol{c}}_{ap,i}\hat{\bar{e}}_i(t) - \bar{A}_{ap,i}^T\boldsymbol{\lambda}_i(t) \tag{43}$$

$$\bar{v}_i(t) = -\frac{1}{r_i}\bar{\boldsymbol{b}}_{ap,i}^T\boldsymbol{\lambda}_i(t) \tag{44}$$

$$\boldsymbol{\lambda}_i(t_f) = P_{f,i}\bar{\boldsymbol{x}}_{ap,i}(t_f) + \nu_{f,i}\bar{\boldsymbol{c}}_{ap,i} \tag{45}$$

$$\bar{\boldsymbol{b}}_{ap,i} = \begin{bmatrix} b_{a,i} \\ \boldsymbol{b}_{fp,i} \end{bmatrix}$$

The optimal predictive input $\bar{v}(t)$ is obtained from (44) by solving (43) with a initial condition $\boldsymbol{\lambda}_i(t_0)$ satisfying (45) with a $\nu_{f,i}$.

Moreover, the initial condition $\boldsymbol{\lambda}_i(t_0)$ satisfying (45) and $\nu_{f,i}$ are obtained as follows from the given conditions (Mizumoto et al., 2018):

$$\begin{bmatrix} \boldsymbol{\lambda}_i(t_0) \\ \nu_{f,i} \end{bmatrix} = \begin{bmatrix} M_{4,i}(t_f) - P_{f,i}M_{2,i}(t_f) & -\bar{\boldsymbol{c}}_{ap,i} \\ \bar{\boldsymbol{c}}_{ap,i}^T M_{2,i}(t_f) & 0 \end{bmatrix}^{-1} \times \begin{bmatrix} P_{f,i}W_{1,i}(t_f) - W_{2,i}(t_f) \\ y_{m,i}(t_f) - \bar{\boldsymbol{c}}_{ap,i}^T W_{1,i}(t_f) \end{bmatrix} \tag{46}$$

Where

$$A_i^* = \begin{bmatrix} \bar{A}_{ap,i} & -\frac{1}{r_i}\bar{\boldsymbol{b}}_{ap,i}\bar{\boldsymbol{b}}_{ap,i}^T \\ -\bar{\boldsymbol{c}}_{ap,i}\bar{\boldsymbol{c}}_{ap,i}^T & -\bar{A}_{ap,i}^T \end{bmatrix}$$

$$M_i(t_f) = \begin{bmatrix} M_{1,i}(t_f) & M_{2,i}(t_f) \\ M_{3,i}(t_f) & M_{4,i}(t_f) \end{bmatrix} = e^{A_i^*(t_f - t_0)}$$

$$\begin{bmatrix} \boldsymbol{a}_{1,i}(t_f) \\ \boldsymbol{a}_{2,i}(t_f) \end{bmatrix} = \int_0^{t_f - t_0} e^{A_i^*\tau}\begin{bmatrix} \mathbf{0} & 1 \\ \bar{\boldsymbol{c}}_{ap,i} & \mathbf{0} \end{bmatrix}\begin{bmatrix} y_{m,i}(t_f - \tau) \\ \bar{z}_{2,i}(t_0) \end{bmatrix}d\tau$$

$$W_{1,i}(t_f) = M_{1,i}(t_f)\bar{\boldsymbol{x}}_{ap,i}(t_0) + \boldsymbol{a}_{1,i}(t_f)$$

$$W_{2,i}(t_f) = M_{3,i}(t_f)\bar{\boldsymbol{x}}_{ap,i}(t_0) + \boldsymbol{a}_{2,i}(t_f)$$

The obtained predictive control input $\bar{v}_i(t)$ is the optimal input for the input $\bar{u}_i(t)$. Therefore the practical optimal

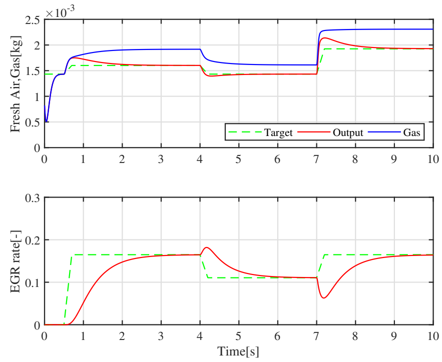

(a) Outputs of controlled system

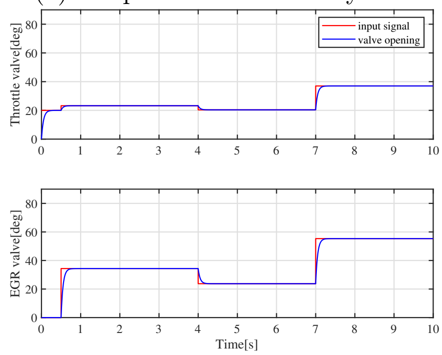

(b) Inputs of controlled system

Fig. 2. Example of the response of general air path system

input $u_i(t)$ is designed as follows for a given interval $t_0 \le t < t_1$ $(t_1 \le t_f)$:

$$u_i(t) = \bar{v}_i(t) - u_{aw,i}(t_0) \quad (t_0 \le t < t_1 \le t_f) \tag{47}$$

4. VALIDATION THROUGH NUMERICAL SIMULATION

The effectiveness of the proposed method is validated through numerical simulations for a air path system given in the section 2.

In the simulation, it supposed that the outputs (fresh air mass, EGR rate) can be measured and available. The inputs (throttle valve angle, EGR valve angle) have mechanical delays modelled by a first order delay dynamics and they are saturated as $\theta_{th}, \theta_{EGR} \in [0, 80]$[deg]. Moreover, the control starts from a steady-state. The considered air path system is assumed to be unknown.

Figure 2 shows the general response of the considered air path system given in the section 2. The response of the fresh air mass into the intake manifold shows overshoot due to the slow response of the EGR. The objective of the control is to prevent the overshoot of the fresh air mass and keep the EGR rate adequately.

In oder to design the control system with PFCs, we first identify the nominal linear model of the considered system by using the Prony-method (Iwai et al., 2003) around a steady state. The identified model is utilized to design the PFC via model-based-design strategy(Mizumoto et al., 2010) so that it allows to obtain not so exact model. If we wonted to use the model for output prediction, we would require an exact and accurate model of the considered air path system.

The nominal models of each subsystem was obtained as follows:

$$G_{nom,11}(s) = \frac{15.3s + 359.4}{s^4 + 216.2s^3 + 1.915e04s^2 + 7.149e05s + 8.261e06}$$

$$G_{nom,22}(s) = \frac{1.531s + 5.961}{s^4 + 27.05s^3 + 239.9s^2 + 793.7s + 827.2}.$$

The PFCs for output estimator of each subsystem are designed as follows by model-based-design strategy using the nominal models:

$$H_{est,i}(s) = G_{est,i}(s) - G_{nom,ii}(s) \ , \tag{48}$$

where

$$G_{est,1}(s) = \frac{10^{-8}}{s + 10^{-3}}, \ G_{est,2}(s) = \frac{10^{-8}}{s + 10^{-4}}. \tag{49}$$

are the ideal augmented systems that satisfy Assumption 1.

The design parameters for the proposed controller were set as

$$k_{1,1} = 10^4 \ , k_{1,2} = 10^2 \ , a_{aw,1} = 10^2$$
$$r_1 = 10^{-6} \ , P_{f,1} = 10^{-5} I$$
$$k_{1,2} = 5 \times 10^2 \ , k_{2,2} = 10^2 \ , a_{aw,2} = 5 \times 10^2$$
$$r_2 = 10^{-5} \ , P_{f,2} = 1I \ , t_f = 5[\text{ms}].$$

Fig. 3 shows simulation results of the method without the anti-windup filter and Fig. 4 shows the results of the proposed method with anti-windup filter, respectively. Figure (a) of each result shows the fresh air mass and the total amount of gas, which is the sum of the fresh air and exhaust gas from EGR, and EGR rate. Figure (b) of each result shows control inputs (throttle valve angle and EGR valve angle) and the obtained actual valve angles of the controlled system.

The results without anti-windup compensation shown in Fig. 3 indicate that the outputs oscillate due to the control inputs saturation. Since the method does not consider the input saturation, it calculates too large inputs, and the input saturation did not converge. As a result, the EGR valve angle oscillates and this affects the EGR performance. On the other hand, the results of the proposed method shown in Fig. 4 shows much better performance without oscillation and the outputs tracked to the reference signal accurately. Furthermore, the fresh air does not have overshoot.

5. CONCLUSION

In this paper, a control of an engine air path system was considered by proposing an anti-windup output predictive control. In the considered air path system, for the mechanical restriction on the input valve angle range, there exists an input saturation. A new output predictive control taking the input saturation into consideration was provided. The effectiveness of the proposed method was confirmed through numerical simulations for a two-input/two-output uncertain system.

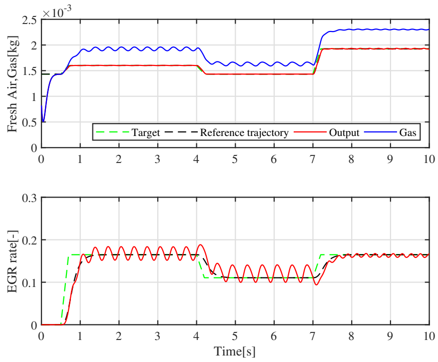

(a) Outputs of controlled system

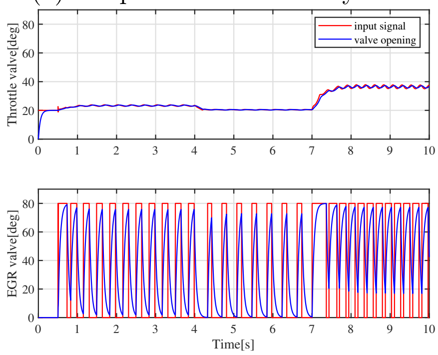

(b) Inputs of controlled system

Fig. 3. Simulation results of the method without anti-windup compensation

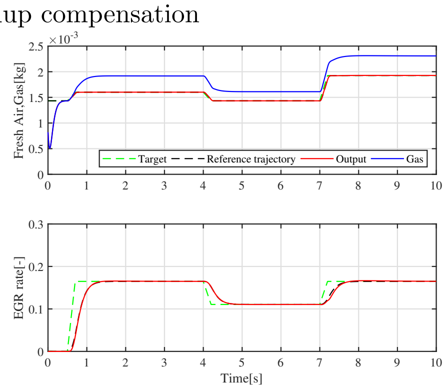

(a) Outputs of controlled system

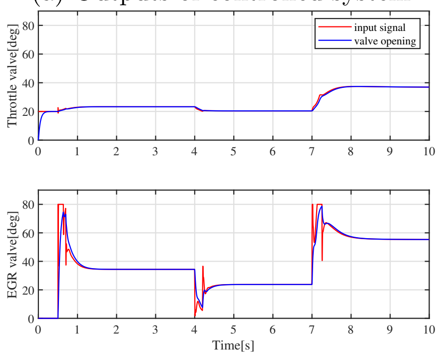

(b) Inputs of controlled system

Fig. 4. Simulation results of the proposed method

ACKNOWLEDGEMENTS

This work is the result of a collaborative research program with the Research association of Automotive Internal Combustion Engines (AICE) for fiscal year 2020. The authors gratefully acknowledge the concerned personnel.

REFERENCES

Clarke, D., Mohtadi, C., and Tuffs, P. (1987). Generalized predictive control - part 1. the basic algorithm. *Automatica*, 23(2), 137–148.

Ferreau, H.J., Ortner, P., Langthaler, P., del Re, L., and Diehl, M. (2007). Predictive control of a real-world diesel engine using an extended online active set strategy. *Annual Reviews in Control*, 31, 293–301.

Garcia, C., Prett, D., and Morari, M. (1989). Model predictive control: Theory and practice -a survey. *Automatica*, 25(3), 335–348.

Gelso, E.R. and Lindberg, J. (2014). Air-path model predictive control of a heavy-duty diesel engine with variable valve actuation. *Proc. of the 19th World Congress IFAC, Cape Town, South Africa. August 24-29*, 3012–3017.

Guzzella, L. and Onder, C. (2020). *Introduction to Modeling and Control of Internal Combustion.* Springer.

Herceg, M., Raff, T., Findeisen, R., and Allg ower, F. (2006). Nonlinear model predictive control of a turbocharged diesel engine. *Proc. of the IEEE CCA 2006*, 2766–2771.

Isidori, A. (1995). *Nonlinear Control Systems.* Springer, 3rd edition.

Iwai, Z., Mizumoto, I., Kumon, M., and Torigoe, I. (2003). Modelling of time delay systems using exponential analysis method. *Proc. of ICCAS 2003*, 2299–2303.

Kekik, B. and Akar, M. (2019). Model predictive control of diesel engine air path with actuator delays. *IFAC PapersOnLine*, 52(18), 150–155.

Kekik, B. and Akar, M. (2020). Model predictive control of diesel engine air path with actuator delays. *IFAC PapersOnLine*, 52(18), 150–155.

Mizumoto, I., Fujii, S., and Mita, H. (2019). Output feedback-based output tracking control with adaptive output predictive feedforward for multiple-input/multiple-output systems. *Industrial & Engineering Chemistry Research*, 58(26), 11382–11391.

Mizumoto, I., Fujimoto, Y., and Ikejiri, M. (2015). Adaptive output predictor based adaptive predictive control with aspr constraint. *Automatica*, 57, 152–163.

Mizumoto, I., Ikeda, D., Hirahata, T., and Iwai, Z. (2010). Design of discrete time adaptive pid control systems with parallel feedforward compensator. *Control Engineering Practice*, 18(2), 168–176.

Mizumoto, I. and Momiki, S. (2018). Augmented anti-windup control for pi control system via aspr based adaptive output feedback with a pfc. *Proc. of 15th International Conference on Control, Automation, Robotics and Vision (ICARCV)*, 650–655.

Mizumoto, I., Murakami, S., and Masuda, S. (2018). Aspr based adaptive output feedback control with an output predictive feedforward input for continuous-time systems. *Proc. of the 57th IEEE Conference on Decision and Control*, 613–619.

Ortner, P., Bergmann, R., Ferreau, H.J., and del Re, L. (2009). Nonlinear model predictive control of a diesel engine airpath. *IFAC Proceedings Volumes*, 42(2), 91–96.